BMC Genomics

RESEARCH Open Access

Transcriptome and DNA methylation analyses provide insight into the heterosis of growth-related traits in hybrid yellow croaker

Dan-Dan Guo[1], Feng Liu[1], Qing-Ping Xie[1], Ting Ye[1], Fu-Liang Wei[1], Bao-Long Niu[1] and Bao Lou[1*]

Abstract

Background Interspecific hybrid combinations of *Larimichthys crocea* × *Larimichthys polyactis* exhibit heterosis in terms of growth traits; however, the molecular regulatory mechanism underlying this phenomenon remains unclear. DNA methylation plays a pivotal role in regulating gene expression and is involved in growth and development processes. In this study, we comprehensively investigated intricate regulatory processes by integrating transcriptome and methylome datasets from brain, liver, and muscle tissues.

Results We analyzed a total of 72 sequence datasets, including transcriptome and genome-wide DNA methylome data, from 36 tissue samples using LC, LP, LPC and LCP. We elucidated the distinct expression patterns of these four populations and examined their interactions with DNA methylation. Our findings revealed diverse DNA methylation profiles and demonstrated a greater number of hypo-DMRs in hybrid yellow croakers than in their parental lines. The majority (86 ~ 92%) of these DMRs were observed within the CG context. Moreover, we found that most DMRs were located within promoter regions as well as exons and introns. A total of 1288 DMEGs were identified through correlation analysis between DNA methylation and transcriptional activity. Functional enrichment analysis revealed that most of the DMEGs were significantly enriched in pathways related to the protein export pathway, proteasome, terpenoid backbone biosynthesis, ubiquitin-mediated proteolysis, autophagy-other pathway. Furthermore, we screened candidate growth-related genes, such as *stat2*, *capn2*, *akt1*, *mTOR*, and *mef2aa*. Among these, the expression levels of *capn2*, *mTOR*, and *akt1* exhibited a positive correlation with DNA methylation levels, whereas the expression levels of *stat2* and *mef2aa* showed a negative correlation. These findings suggest that alterations in DNA methylation patterns may promote growth advantages in hybrid yellow croaker by modulating the expression of these genes.

Conclusions Epigenetic changes exert distinct influences on genes related to growth heterosis. The presented data establish a foundation for comprehending the epigenetic and transcriptomic alterations underlying the growth of hybrid yellow croaker, thereby providing preliminary insights into the molecular mechanisms of growth heterosis. These findings have significant implications for breeding programs aimed at enhancing yellow croaker production.

Keywords *Larimichthys crocea*, *Larimichthys polyactis*, Hybrid yellow croaker, Transcriptome, Growth trait, DNA methylation

*Correspondence:
Bao Lou
loubao6577@163.com
[1]State Key Laboratory for Managing Biotic and Chemical Threats to the Quality and Safety of Agro-products, Institute of Hydrobiology, Zhejiang Academy of Agricultural Sciences, Hangzhou 310021, China

Background

Hybridization, which encompasses numerous cross combinations that exhibit heterosis [1], is extensively employed in the field of aquaculture. The small yellow croaker (*Larimichthys polyactis*, LP) primarily inhabits the Bohai Sea, Yellow Sea, and East China Sea, while the large yellow croaker (*Larimichthys crocea*, LC) predominantly occurs in the Bohai Sea, East China Sea and South Sea [2]. In 2022, the total national output reached 257,683 tons [3], making them two important economic fishes in offshore China [4]. Since 2016, we have successfully bred the fast-growing strains LPC (*Larimichthys polyactis* ♀ × *Larimichthys crocea* ♂) and LCP (*Larimichthys crocea* ♀ × *Larimichthys polyactis* ♂) through interspecific hybridization. At 12 months of age, LCP lines exhibited the highest growth rate, demonstrating overparent heterosis, while LPC lines displayed an intermediate growth rate between the parents, indicating midparent heterosis. Heterosis, commonly observed in hybrids, refers to the phenomenon where hybrid offspring exhibit superior traits compared to their parents, such as enhanced growth, disease resistance, and improved muscle nutritional quality. This phenomenon has significant applications in aquaculture, particularly for species like the yellow croaker, where hybridization has been shown to enhance growth rates and production efficiency. Maximizing the benefits of heterosis is the primary objective in crossbreeding. However, the molecular basis of growth heterosis in hybrid yellow croakers remain poorly understood. Understanding the molecular mechanism of growth-related traits in hybrid yellow croaker and breeding fast-growing varieties is crucial for enhancing output and economic value. Studies suggest that gene expression and DNA methylation play pivotal roles in regulating heterosis. Numerous differentially expressed genes (DEGs) that exhibited differential methylation (DMEGs) associated with heterosis have been identified in *Haliotis diversicolor* hybrids, Dorper×Small Tailed Han crossbreds, and hybrid rice through gene expression and epigenetic analyses [5–7]. However, the regulatory mechanism by which DNA methylation influences gene expression to enhance growth performance in hybrid yellow croaker has not been determined. This study aims to examine the transcriptomic and DNA methylation profiles of hybrid and parental yellow croakers to uncover the molecular mechanisms underlying their superior growth characteristics.

DNA methylation is one of the hallmarks of epigenetic mechanisms and is involved in pretranscriptional regulation. Alterations in the level of methylation in hybrid offspring further impact transcription levels, thus contributing to the development of heterosis [8, 9]. A previous study showed that *Haliotis diversicolor* hybrids have lower levels of whole-genome methylation, which results in more active gene transcription through epigenetic regulation. These changes ultimately lead to phenotypic differences through a series of physiological and biochemical processes, such as translation and metabolic pathways [5]. Variation was observed in the DNA methylation patterns of inter-subspecific hybrid rice, which negatively regulate gene expression. The differentially expressed genes associated with photosynthesis functions were significantly enriched, influencing flag leaf gene expression and heterosis [7].

In the present study, the analysis of phenotypic traits revealed significant heterosis during the growth of hybrid yellow croaker. To investigate the role of gene expression and DNA methylation in the development of growth heterosis, we first performed RNA-seq and Whole Genome Bisulfite-Seq (WGBS) analyses of brain, liver, and muscle tissues from 36 yellow croakers belonging to four populations (LC, LP, LPC, and LCP). Moreover, we screened DEGs, differentially methylated genes (DMGs), and DMEGs between the hybrid offspring and their parental lines. We analyzed the correlation between gene expression and apparent regulation while exploring the key metabolic pathways underlying DMEGs enrichment in growth. These results provide valuable insights into the underlying molecular mechanisms driving heterosis at both the transcriptional and DNA methylation levels and may lead to enhanced genetic improvement of growth traits in yellow croaker.

Methods

Animal and tissue collection

Two parental lines, *Larimichthys crocea* and *Larimichthys polyactis*, and the interspecific hybrids LPC and LCP were used in this study. All the experimental animals were sourced from Xiangshan Harbor Aquatic Seedling Co., Ltd., Ningbo, China. The fry of the hybrids and their parental lines were raised under the same conditions. During the breeding period, aquatic compound feed was provided. The nutritional composition of this feed includes crude protein ≥ 35.00%, crude fat ≥ 3.00%, coarse fibre ≤ 8.00%, crude ash ≤ 16.00%, moisture ≤ 12.00%, total phosphorus ≥ 0.50%, and lysine ≥ 1.70%. After 12 months of age, body weight and body length were measured for the four lines, and analysis of variance (ANOVA) was conducted to assess heterosis in hybrid yellow croaker. After the experimental fish were anesthetized using tricaine methanesulfonate (MS-222) (Sigma, USA), tissues, including the brain, liver, and muscle, from each line were collected and immediately frozen in liquid nitrogen for subsequent RNA or DNA extraction. For each tissue, three replicates were performed, RNA-Seq and WGBS were performed.

mRNA library construction and sequencing

For RNA-Seq, total RNA was extracted from 36 tissue samples using TRIzol (Invitrogen, USA) according to the manufacturer's instructions. The concentration of RNA was assessed using a NanoDrop (Thermo Fisher Scientific, USA), and the quality was evaluated on an Agilent 2100 bioanalyzer (Thermo Fisher Scientific, USA). All samples with an RNA integrity number (RIN) ≥ 7.0 and a 28 S/18S ratio ≥ 1.5 were used to prepare sequencing libraries to ensure high-quality sequencing data. mRNA was purified using oligo (dT)-attached magnetic beads and fragmented into small pieces. cDNA was synthesized using random hexamer-primed reverse transcription. Subsequently, A-Tailing Mix and RNA Index Adapters were added and incubated for end repair. The cDNA fragments obtained from the previous step were amplified by PCR, and the double-stranded PCR products were heated, denatured and circularized by the splint oligo sequence to obtain the final library. The final library was amplified with phi29 to generate DNA nanoballs (DNBs), which included more than 300 copies of one molecule. The DNBs were loaded into the patterned nanoarray and sequenced on the BGIseq500 platform (BGI-Shenzhen, China), which generated 100 bp paired-end reads.

Bioinformatics processing and transcriptome data analysis

Clean reads were obtained by removing reads containing a sequencing adapter, reads with a high ratio (more than 20%) of low-quality bases (base quality less than or equal to 5), and reads with a high ratio (more than 5%) of unknown bases ('N' base) from the raw data with SOAPnuke (v1.5.2) [10]. The clean reads for each sample were aligned to the *Larimichthys crocea* reference genome using HISAT2 (v2.0.4) [11]. Gene expression levels were quantified in terms of the fragments per kilobase of transcript per million fragments mapped (FPKM) by RSEM (v1.2.12) [12]. Differential expression analysis was performed using DESeq2 (v1.4.5) [13], with the criterion of a *P*-value ≤ 0.05 as the threshold for significance assessment. To gain insight into the phenotypic changes, Gene Ontology (GO) and Kyoto Encyclopedia of Genes and Genomes (KEGG) enrichment analyses of annotated differentially expressed genes were performed using Phyper based on a hypergeometric test. The significance levels of terms and pathways were corrected by the Q value with a rigorous threshold (Q value ≤ 0.05) following the Bonferroni method [14].

DNA methylation library preparation and sequencing

Construction of the DNA methylation library used the same samples as RNA-Seq. Libraries were prepared according to the following protocol. Briefly, genomic DNA was isolated using the DNeasy Blood & Tissue Kit (Qiagen, Germany). The integrity of the DNA was assessed using agarose gel electrophoresis. Typically, genomic DNA exhibits a distinct high-molecular-weight band. The purity and concentration of the DNA were measured using a Qubit® DNA Assay Kit in a Qubit® 2.0 Fluorometer (Life Technologies, USA) and a NanoDrop spectrophotometer. A total of 100 ng of genomic DNA spiked with 0.5 ng of lambda DNA was fragmented by sonication to 200 ~ 300 bp with a Covaris S220 column, followed by end repair, 3'-adenylation and ligation with a methylated adapter. Subsequently, these DNA fragments were treated with bisulfite using an EZ DNA Methylation-GoldTM Kit (Zymo Research, USA), followed by PCR amplification to generate the library. After the library quality was assessed on an Agilent 2100 bioanalyzer, paired-end sequencing of the samples was performed on an Illumina NovaSeq platform (Illumina, CA, USA).

Methylation calculation and differentially methylated analysis

The raw reads were trimmed through fastp (fastp 0.20.0) to filter out low-quality and adapter sequences. The remaining reads that passed all the filtering steps were counted as clean reads, and all subsequent analyses were based on these results. These clean reads were subsequently mapped to the *Larimichthys crocea* reference genome using Bismark software (version 0.16.3) [15]. Alignments were performed to identify the methylated cytosines using the Bismark methylation extractor with default parameters. The numbers of methylated and unmethylated reads were calculated. The methylation level was defined as the number of methylated reads (mC) divided by the total number of methylated reads (mC) and unmethylated reads (umC) at the same positions in the reference genome [16]. The identification of differentially methylated regions (DMRs) was performed using DSS software [17–19]. Based on the distribution of DMRs throughout the genome, we defined the genes associated with DMRs as genes whose gene body, from the transcription start sites (TSS) to the transcription termination site (TES), or promoter region (upstream 2 kb from the TSS) overlapped with the DMRs. Finally, GO and KEGG enrichment analyses were conducted using the GOseq R package [20] and KOBAS software [21], respectively.

Results

Evaluation of heterosis for growth-related traits in hybrid yellow croaker

As shown in Fig. 1; Table 1, compared with their parents, LCP hybrids exhibited significant heterosis in terms of body weight and body length. The mean body weight of the LCP hybrids (78.14 ± 20.36) was significantly greater than that of the LC (60.30 ± 23.66, 29.59%) and

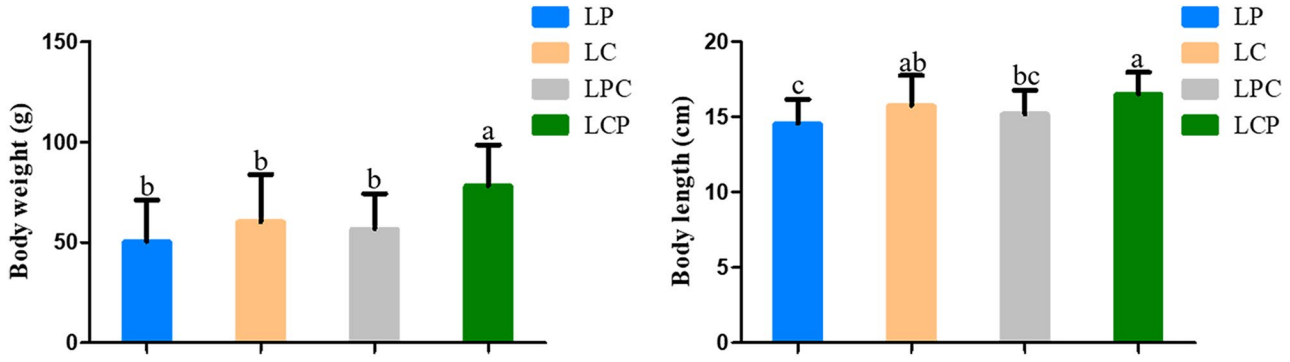

Fig. 1 Growth comparison of 12-month-old hybrid yellow croaker and their parents. Different letters indicate significant differences ($P < 0.05$)

Table 1 Growth comparison of 12-month-old hybrid yellow croaker and their parents

	LP	LC	LPC	LCP
Body weight (g)	50.40 ± 20.69^{b}	60.30 ± 23.66^{b}	56.73 ± 17.59^{b}	78.14 ± 20.36^{a}
Body length (cm)	14.56 ± 1.62^{c}	15.74 ± 2.01^{ab}	15.20 ± 1.60^{bc}	16.50 ± 1.48^{a}

Different letters indicate significant differences ($P < 0.05$)

LP (50.40 ± 20.69, 55.04%), and the mean body length of the LCP (16.50 ± 1.48%) was significantly greater than that of the LP (14.56 ± 1.62, 13.32%). Although there were no significant differences in body weight or body length between the LPC hybrids and their parents, their body weight increased by approximately 12.6% compared to that of the female parent LP.

Overview of multi-omics datasets

In total, we constructed 36 mRNA libraries from two different hybrid yellow croaker species and their parents, resulting in the generation of 1610.67 million raw reads. After performing sequence quality control and filtering, a total of 1543.52 million clean reads were obtained, with an average of 42.88 million reads per sample. The clean reads for all the samples were aligned to the *Larimichthys crocea* reference genome, for which the average mapping rate was 90.40% (ranging from 84.28 to 96.1%). Detailed mapping information for each sample is provided in Additional file 1: Table S1.1. We generated a total of 36 WGBS datasets, as described in Additional file 1: Table S1.2. These datasets yielded 2,953,482,636 clean reads (approximately 82041184 per sample), with an average of 48.72% of the clean reads uniquely mapped to the *Larimichthys crocea* reference genome.

We quantified the expression levels of 52,423 transcripts (21430 existing and 30993 novel) in 36 samples and detected a total of 353,262,075 methylated cytosines across these samples. The distribution of methylated cytosines in different region types is shown in Additional file 2: Table S2. Principal component analysis (PCA) of all 36 samples based on transcription and DNA methylation profiles revealed consistent clustering according to tissue type. The correlations for biological replicates showed strong associations; the correlations for the same tissues of different species were relatively weaker, and the correlations for different tissues were the weakest (Fig. 2a). The distributions of mRNA expression levels and DNA methylation levels in all 36 samples are depicted in Fig. 2b. Analysis of the mRNA expression levels revealed no significant differences among the numbers of genes expressed in the same tissues across different species; that is, the hybrid yellow croaker and its parents exhibited no significant "dosage effect".

Defining differential expression patterns of mRNAs between four populations

The counts of the genes expressed in the hybrid yellow croaker and its parents are shown in Additional file 3: Table S3 and Fig. 3. Furthermore, a total of 4250 DEGs were identified in the hybrid yellow croaker (Fig. 4; Additional file 3: Table S4). According to the literature, DEGs are likely related to the development of heterosis [22]. LP and LC served as the control groups, whereas LCP and LPC were the experimental groups. In comparison to those in the control group, we screened (P-value ≤ 0.05) a total of 99 (67 upregulated and 32 downregulated), 197 (140 upregulated and 57 downregulated), 139 (91 upregulated and 48 downregulated) and 197 (139 upregulated and 58 downregulated) DEGs in the LC_Brain vs. LCP_Brain, LP_Brain vs. LCP_Brain, LC_Brain vs. LPC_Brain and LP_Brain vs. LPC_Brain groups, respectively. Similarly, 385 (277 upregulated and 108 downregulated), 645 (424 upregulated and 221 downregulated), 421 (266 upregulated and 155 downregulated) and 579 (341 upregulated and 238 downregulated) DEGs were screened from the LC_Liver vs. LCP_Liver, LP_Liver vs. LCP_Liver, LC_Liver vs. LPC_Liver and LP_Liver vs. LPC_Liver groups, respectively. Additionally, 932 (672 upregulated and 260 downregulated), 608 (443

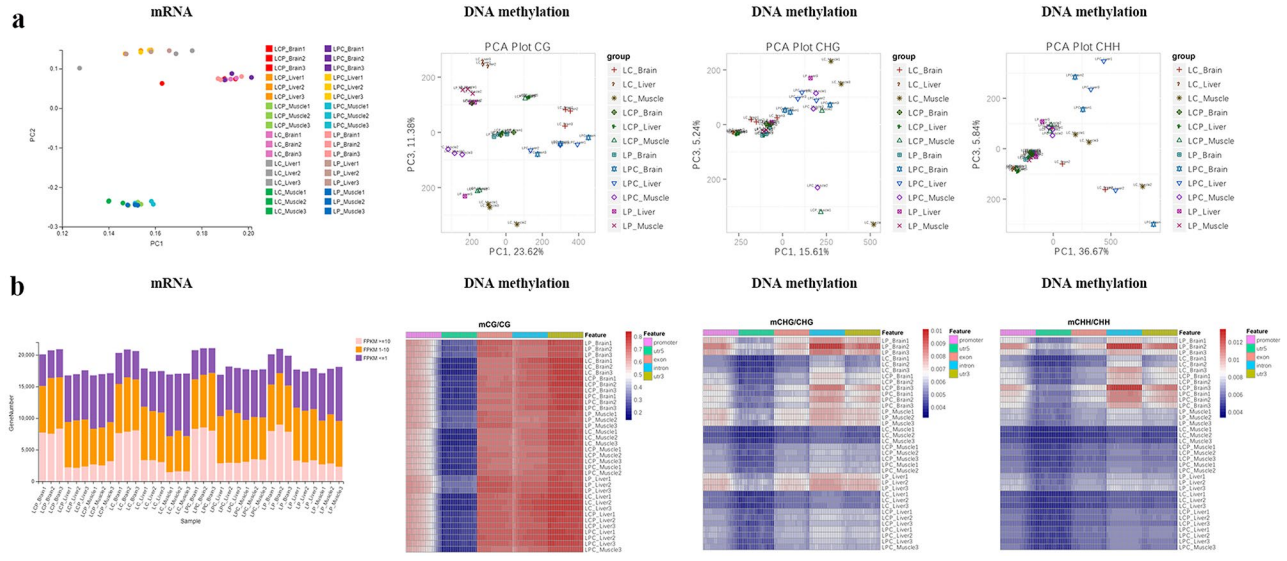

Fig. 2 Gene expression and DNA methylation among samples. **a**. PCA of all 36 samples based on transcription and DNA methylation; **b**. The distribution of gene expression and DNA methylation across different samples

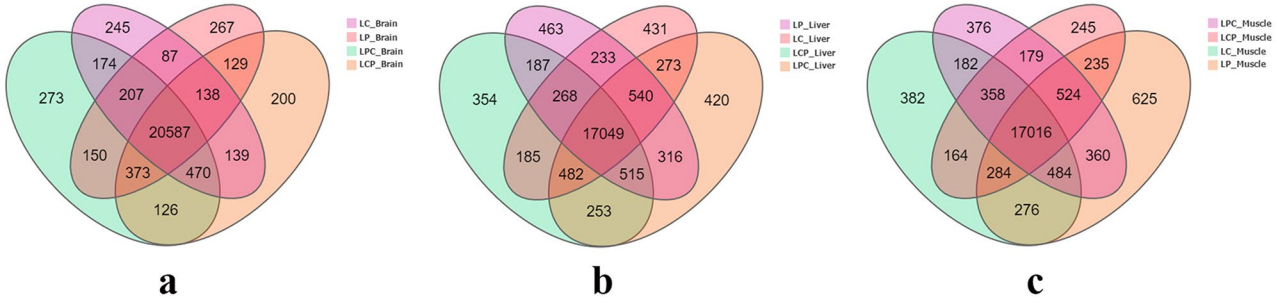

Fig. 3 The number of expressed genes in the hybrid yellow croaker and its parents

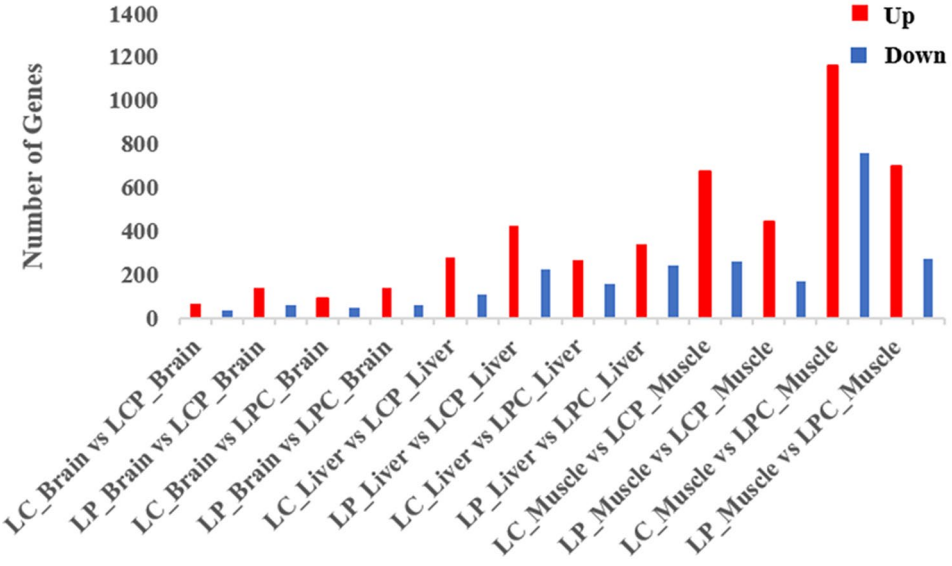

Fig. 4 Differentially expressed gene analysis of hybrid yellow croaker compared to their parental lines

upregulated and 165 downregulated), 1923 (1162 upregulated and 761 downregulated) and 966 (696 upregulated and 270 downregulated) DEGs were screened in the LC_Muscle vs. LCP_Muscle, LP_Muscle vs. LCP_Muscle, LC_Muscle vs. LPC_Muscle and LP_Muscle vs. LPC_Muscle groups, respectively.

The DEGs were annotated to the GO [23] and KEGG [24]. The DEGs in the LCP hybrid triad were classified into three categories: 1421 biological processes, 974 cellular components, and 1407 molecular functions (Additional file 4: Fig. S1a). In contrast, the DEGs in the LPC hybrid triad included 2119 biological processes, 1418 cellular components, and 2056 molecular functions (Additional file 4: Fig. S1b). Notably, there was a remarkable concordance between the results of GO and KEGG analysis for DEGs in both LCP and LPC hybrids. In the biological process category, DEGs were predominantly enriched in "metabolic process", "developmental process" and "growth". For cellular components, most of the DEGs were associated with the terms "cellular anatomical entity" and "protein-containing complex". Among the molecular functions, "cytoskeletal motor activity", "catalytic activity", "transcription regulator activity" and "translation regulator activity" were enriched. The results of KEGG analysis revealed significant enrichment of DEGs in pathways related to "Mitophagy", "PPAR signaling pathway", "Protein processing in endoplasmic reticulum", and "Cellular senescence", as well as pathways related to amino acid synthesis and catabolism (Additional file 4: Fig. S1c, d).

Differentially methylated regions (DMRs) of parents and F1 hybrid genomes

A total of 184,476 and 211,714 DMRs were identified in the LCP and LPC, respectively (Fig. 5a, Additional file 5: Table S5). Different methylation contexts affect the

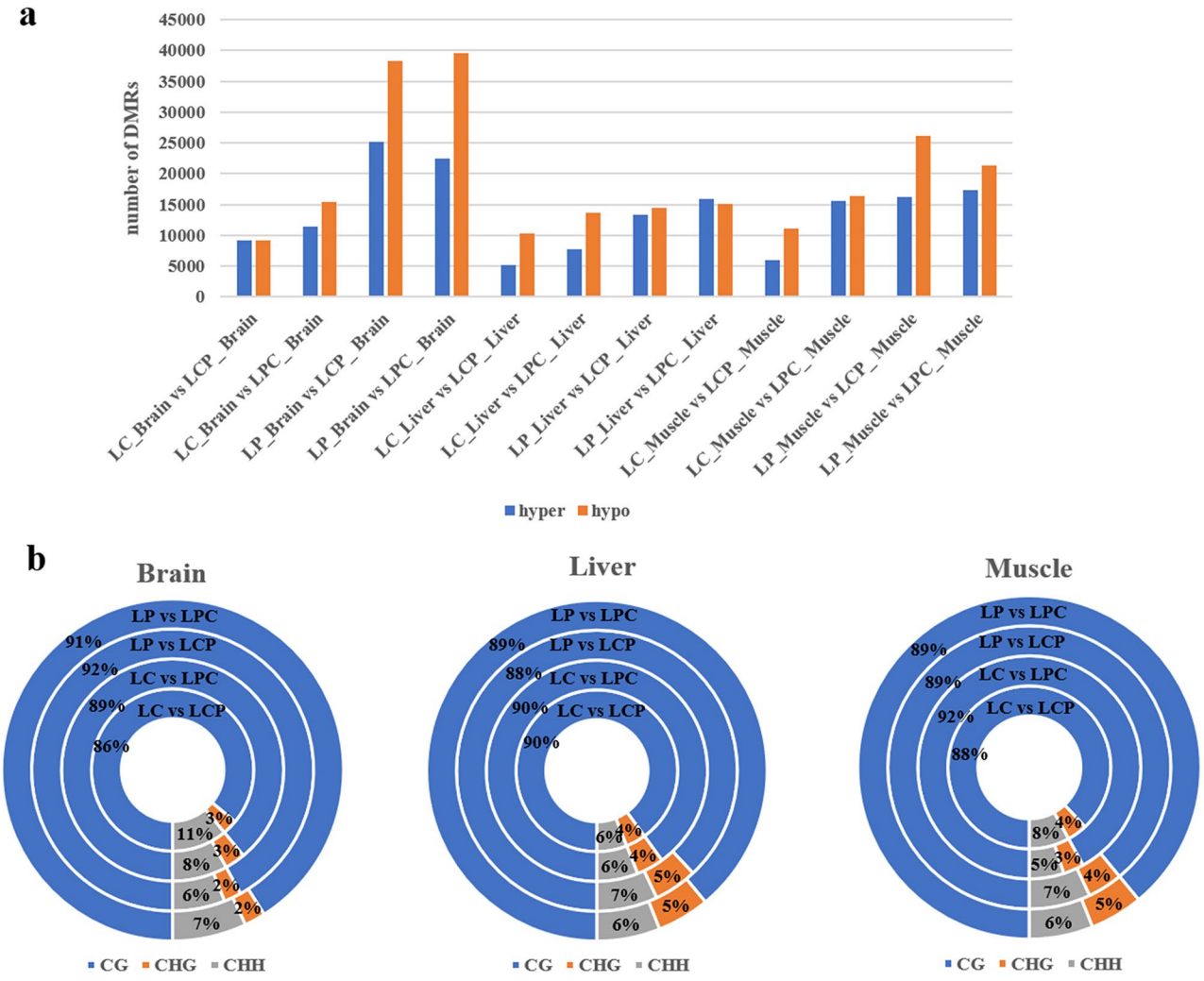

Fig. 5 Characteristics of DMRs in the hybrid yellow croaker. **a**. The number of hyper and hypo-DMRs; **b**. The proportion of 3 types of mC sites within the DMR

number of DMRs. Among these DMRs, 86 ~ 92% were in the CG context (Fig. 5b). Compared with those in the parental lines, 66,642 and 80,423 DMRs were hypermethylated, and 99,003 and 110,002 DMRs were hypomethylated in the CG context in the LCP and LPC populations, respectively. For the CHG context, 6377 (2043 hyper and 4334 hypo) and 6936 (2223 hyper and 4713 hypo) DMRs were identified in the LCP and LPC, respectively. In addition, 12,454 (6265 hyper and 6189 hypo) and 14,353 (7639 hyper and 6714 hypo) DMRs were identified in the LCP and LPC, respectively, in the CHH context.

DMRs exhibited different distributions in the genome (Fig. 6). To investigate the genome-wide methylation pattern, we examined methylation levels in various genetic structural regions, including the promoter, 2 kb region upstream of the TSS, 5'-UTR, exon, intron, 3'-UTR, and 2 kb region downstream of the TES. The results revealed that most of the DMRs were located in the promoter and coding regions of genes, including exons and introns, while their distribution in other noncoding regions was relatively rare. Furthermore, analysis of DMR methylation levels demonstrated a greater number of highly methylated DMRs in LC and LP than in LCP and LPC (Additional file 6: Fig. S2-4).

Comparative analysis of DNA methylation and gene expression between parents and F1 hybrid genomes

Integrated analysis of the overlap between the DMGs and DEGs was conducted at the CG, CHG, and CHH contexts to determine the potential relationship between DNA methylation and gene expression. As a result, we detected 9 DMEGs in the LC_Brain vs. LCP_Brain, 21 DMEGs in the LP_Brain vs. LCP_Brain, 13 DMEGs in the LC_Brain vs. LPC_Brain, and 22 DMEGs in the LP_Brain vs. LPC_Brain (Additional file 7: Fig. S5, Table S6). In the comparisons of LC_Liver vs. LCP_Liver, LP_Liver vs. LCP_Liver, LC_Liver vs. LPC_Liver, and LP_Liver vs. LPC_Liver, a total of 58, 158, 50, and 134 DMEGs were identified. Similarly, in the comparisons of LC_Muscle vs. LCP_Muscle, LP_Muscle vs. LCP_Muscle, LC_Muscle vs. LPC_Muscle, and LP_Muscle vs. LPC_Muscle, a total of 174, 176, 464, and 281 DMEGs, respectively, were identified. After removing overlapping DMEGs, 1288 DMEGs were obtained for subsequent functional analysis.

GO and KEGG annotations of DMEGs

To further investigate the potential role of DNA methylation in gene regulatory networks during individual growth and development, we carried out GO enrichment analysis on the 1288 DMEGs (Fig. 7a; Additional file 8: Table S7.1). The results showed that 123 functional categories were annotated to cellular components, including ribonucleoprotein complex, cytoplasm, cytoplasmic part, endoplasmic reticulum, and the endomembrane system. 405 functional categories were primarily associated with biological processes such as peptide metabolic process, oxidation–reduction process, protein targeting, protein localization to endoplasmic reticulum, protein localization to membrane, establishment of protein localization to membrane, and cellular amide metabolic process. Additionally, 267 functional categories were enriched in molecular function, mainly ubiquitin-protein transferase activity, ubiquitin-like protein transferase activity, oxidoreductase activity, NAD or NADP as acceptor, and oxidoreductase activity.

The enrichment of the top 20 KEGG pathways of the DMEGs revealed that the protein export pathway, proteasome pathway, terpenoid backbone biosynthesis pathway, ubiquitin-mediated proteolysis pathway, and autophagy-other pathway were significantly enriched (Fig. 7b; Additional file 8: Table S7.2). Based on KEGG enrichment analysis, we identified five key genes associated with growth and development: the neuroendocrine factor *stat2*; the protein synthesis- and degradation-related genes *capn2* and *akt1*; the appetite-related signaling molecule *mTOR*; and the muscle growth regulatory factor *mef2aa*. These findings underscore the crucial roles of DNA methylation regulation in individual growth and development.

Discussion

Hybridization is an effective tool for genetic improvement in aquaculture, enabling the creation of hybrids with heterosis through the integration of genomes from different parental species [1]. In terms of heterosis of growth traits, the improved hybrid bream (BTBB) derived from a hybrid lineage of *M. amblycephala* (♀) × *C. alburnus* (♂) exhibited a faster growth rate than did its male parent [25]. The average weight of 12-month-old WRs (white crucian carp ♀ × red crucian carp ♂) closely approached that of white crucian carp and significantly surpassed that of red crucian carp by 26.42% [26]. Similarly, this type of growth heterosis was also observed in reciprocal crosses between *Channa argus* and *Channa maculate* [27]. However, it remains uncertain whether these hybrids can combine dominant characteristics from both parents. In this study, we first assessed the growth of 12-month-old hybrid yellow croaker. The growth rate of LCP was 55.04% and 29.59% greater than that of paternity (LP) and maternity (LC), respectively. Although no statistically significant difference was observed, LPC demonstrated an approximately 12.6% greater body weight gain than did the female parent LP. These findings indicate significant heterosis in terms of growth traits for both LCP and LPC hybrids, providing valuable material for investigating the molecular mechanisms underlying heterosis.

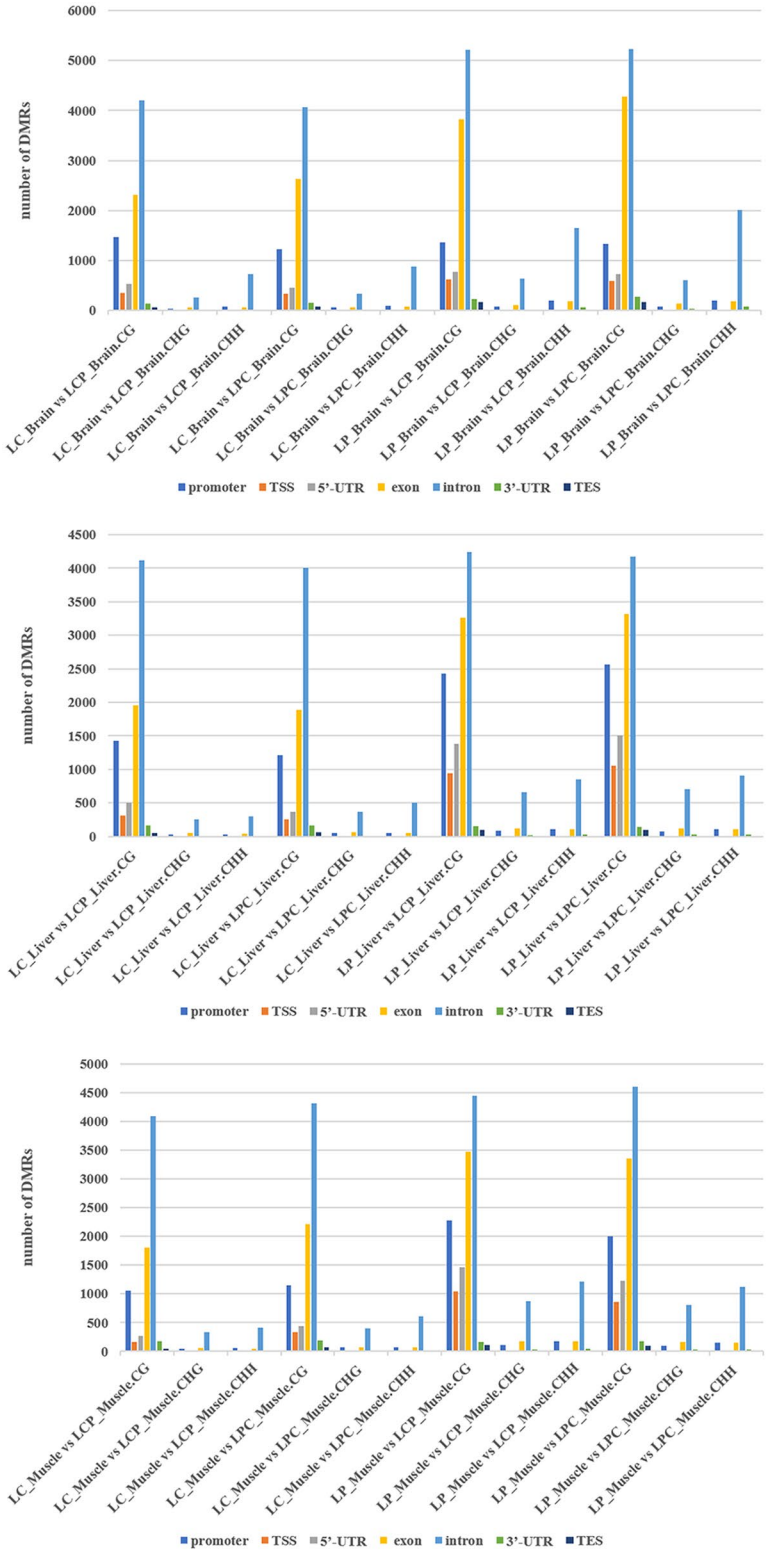

Fig. 6 The distribution of DMRs throughout the genome

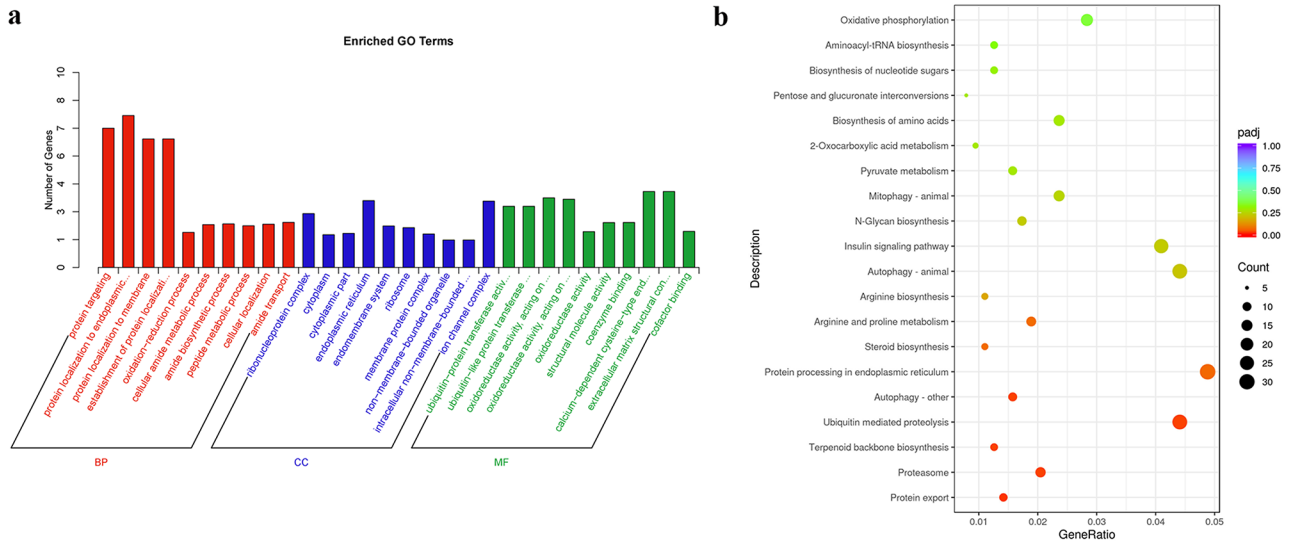

Fig. 7 The functional annotation of DMEGs. **a** GO annotation of DMEGs; **b** KEGG pathway enrichment of DMEGs

Hybridization may contribute to the development of heterosis by activating or inhibiting the expression of certain genes in hybrids [28]. Transcriptome analysis revealed a high degree of similarity in the overall gene expression profiles between hybrids and their parental lines, with only a small proportion of genes exhibiting significantly different expression levels. These findings are consistent with previous studies investigating heterosis resulting from hybridization in mandarin fishes, grouper, pufferfish, and other aquaculture species [29–31]. These DEGs provided valuable clues for elucidating the development of growth heterosis. After functional annotation and bioinformatics analysis, DEGs were found to be related to the following categories: "metabolic process", "developmental process", "growth", "cytoskeletal motor activity", "transcription regulator activity" and "translation regulator activity". In addition, these DEGs were significantly enriched in multiple pathways involved in "Mitophagy", "PPAR signaling pathway", "Protein processing in endoplasmic reticulum", and "Cellular senescence", as well as pathways related to amino acid synthesis and catabolism. These findings indicated that the screened DEGs may participate in the regulatory processes of growth heterosis in hybrid yellow croaker.

In addition to genetic regulation, epigenetic modifications, such as DNA methylation, have been confirmed to play a role in the development of heterosis [9, 32, 33]. In our study, we observed that the total relative methylation level was lower in hybrid yellow croaker compared to its parental lines. These hypo-DMRs may lead to the activation of key growth-related genes that are suppressed in the parental lines. For instance, genes involved in cell proliferation and growth hormone signaling pathways. This finding was consistent with previous studies on DNA methylation in other hybrid species, including plants and livestock, where genomic DNA hypomethylation may be associated with heterosis. Specifically, the role of hypo-DMRs in facilitating the expression of beneficial traits has been observed in several hybrid systems. For example, compared with those in the small-tailed Han group, DNA methylation in the LDM was lower, and DMRs were more prone to hypomethylation in the crossbred group [34]. In maize hybrids, total relative methylation levels were lower than corresponding midparent values, and a greater number of demethylation events were inferred for the hybrids [35]. Similarly, "Mohe" hybrid tilapia displayed lower methylation levels than did their parental progenies [36]. These comparisons suggest that the epigenetic regulation of gene expression through DNA methylation is a conserved mechanism underlying heterosis across different species. Our study provides new insights into the role of epigenetic modifications in mediating heterosis and identifies potential targets for improving growth performance in hybrid breeding programs.

In this study, we conducted a comprehensive analysis of DNA methylation and gene expression data and identified 1288 genes whose methylation and expression levels differed. The DMRs were mainly distributed in the promoter, intron and exon regions of genes but were rarely distributed in other noncoding regions. Among the 1288 genes obtained, 5 closely associated with growth and development were screened: the neuroendocrine factor *stat2*; the protein synthesis- and degradation-related genes *capn2* and *akt1*; the appetite-related signaling molecule *mTOR*; and the muscle growth regulatory factor *mef2aa*. *Capn2* is a member of the calpain family, and the calcium-activated cysteine protease m-calpain encoded

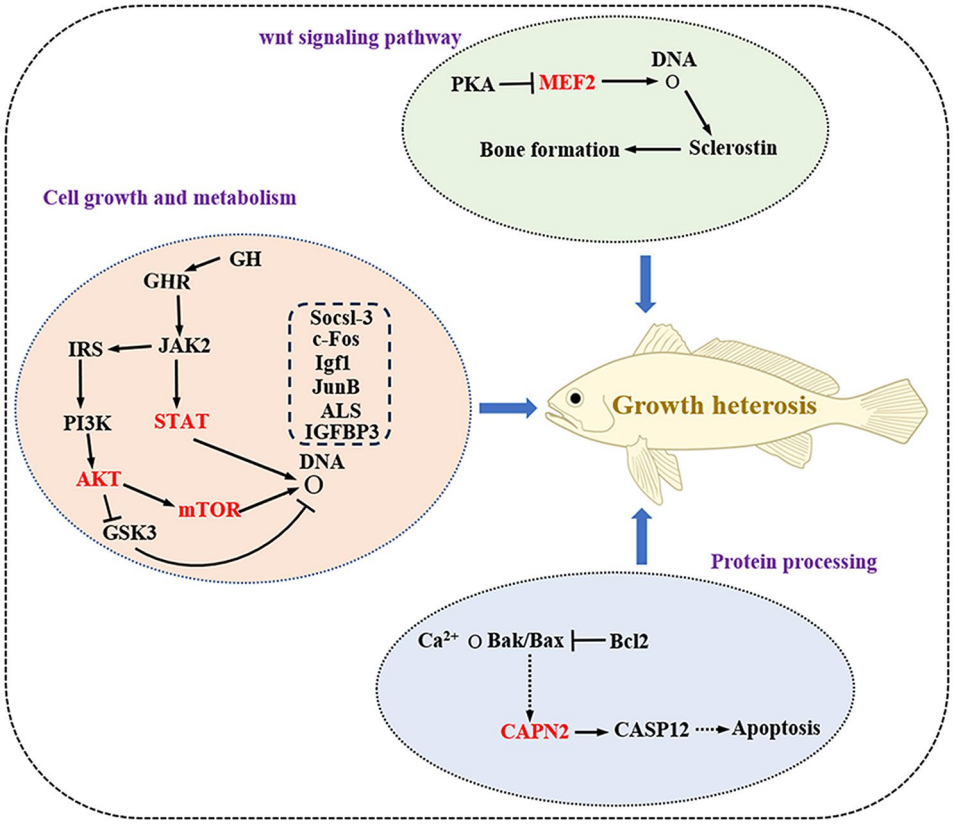

Fig. 8 The pathway of DMEGs regulated growth heterosis

by it plays a pivotal role during the earlier stages of myogenesis, particularly during fusion [37]. Both *mTOR* and *akt1* are involved in the *mTOR* signaling pathway. *mTOR* is a highly conserved serine-threonine kinase that plays a pivotal role in the regulation of feeding. It controls growth and development by integrating nutrient signals with hormonal signals [38]. The results of this study demonstrated a positive correlation between the expression levels of *capn2*, *mTOR*, and *akt1* and DNA methylation levels. This finding suggested that DNA methylation within these regions may promote gene transcription and thereby participate in the growth of hybrid progeny. *Mef2aa*, a crucial member of the myocyte enhancer factor family, plays an important role in the process of muscle genesis and regeneration [39]. *Stat2*, a member of the STAT family, exerts a significant influence on cell proliferation [40]. Our results showed that the expression levels of *stat2* and *mef2aa* were negatively correlated with DNA methylation levels, suggesting that decreased DNA methylation may promote the binding of specific transcription factors, thereby improving transcription efficiency and gene expression. According to the above analysis, the growth heterosis of hybrid yellow croakers was jointly regulated by neuroendocrine factors, protein synthesis- and degradation-related genes, appetite-related signaling molecules, and muscle growth regulatory factors (Fig. 8). However, further investigations are needed to elucidate the regulatory mechanism by which DNA methylation influences the expression of these genes and to explore the impact of these modifications on hybrid yellow croaker growth.

Conclusions

Overall, the present investigation systematically explored the transcriptional profile and DNA methylation patterns of hybrid yellow croaker and its parents. We screened DMEGs and were found to be closely related to growth heterosis. Our findings shed light on the intricate regulatory networks of gene expression and DNA methylation during growth and development. These results enrich the regulatory network related to growth and contribute to elucidating the molecular mechanisms driving heterosis. The implications of this study for aquaculture are significant. By uncovering genetic and epigenetic factors contributing to heterosis, these findings can be applied to improve breeding programs for hybrid yellow croaker and other commercially important fish species, potentially enhancing production efficiency. Although this study offers a comprehensive analysis of heterosis at the molecular level, further research is necessary to validate the functional roles of the key genes identified. A limitation of this study was the absence of validation for the

differential expression of key genes identified. In future studies, we plan to confirm the expression patterns of these genes using qRT-PCR and Western blot techniques and verify the correlation between gene expression and function through functional assays. Additionally, further research is required to explore how environmental factors interact with genetic and epigenetic mechanisms to influence heterosis, as well as to investigate the potential of genetic modification techniques to optimize hybrid traits.

Abbreviations

LP	Larimichthys polyactis
LC	Larimichthys crocea
LPC	Larimichthys polyactis ♀ × Larimichthys crocea ♂
LCP	Larimichthys crocea ♀ × Larimichthys polyactis ♂
WGBS	Whole Genome Bisulfite-Seq
DEGs	Differentially expressed genes
DMGs	Differentially methylated genes
DMEGs	Differentially expressed genes that exhibited differential methylation
RIN	RNA integrity number
FPKM	Fragments per kilobase of transcript per million fragments mapped
DMRs	Differentially methylated regions
ANOVA	Analysis of Variance
PCA	Principal component analysis
GO	Gene Ontology
KEGG	Kyoto Encyclopedia of Genes and Genomes
TSS	Transcription start sites
TES	Transcription termination site

Supplementary Information

The online version contains supplementary material available at https://doi.org/10.1186/s12864-025-11248-y.

Supplementary Material 1: Additional file 1: Table S1. The transcriptome and DNA methylation sequencing data. Table S1.1 Summary of the transcriptome sequencing data. Table S1.2 Summary of DNA methylation sequencing data.

Supplementary Material 2: Additional file 2: Table S2. The distribution of methylated cytosines in different regions.

Supplementary Material 3: Additional file 3: Table S3. Normalized expression levels of genes detected in hybrid yellow croaker and its parents. Table S3.1 Normalized expression levels of genes detected in the brain tissue of LCP and its parents. Table S3.2 Normalized expression levels of genes detected in the brain tissue of LPC and its parents. Table S3.3 Normalized expression levels of genes detected in the liver tissue of LCP and its parents. Table S3.4 Normalized expression levels of genes detected in the liver tissue of LPC and its parents. Table S3.5 Normalized expression levels of genes detected in the muscle tissue of LCP and its parents. Table S3.6 Normalized expression levels of genes detected in the muscle tissue of LPC and its parents. Table S4. The expression levels of DEGs identified in the hybrid yellow croaker. Table S4.1 The expression levels of DEGs identified in the comparison of LC_Brain vs. LCP_Brain. Table S4.2 The expression levels of DEGs identified in the LP_Brain vs. LCP_Brain comparison. Table S4.3 The expression levels of DEGs identified in the comparison of LC_Brain vs. LPC_Brain. Table S4.4 The expression levels of DEGs identified in the LP_Brain vs. LPC_Brain comparison. Table S4.5 Expression levels of DEGs identified in the comparison of LC_Liver vs. LCP_Liver. Table S4.6 Expression levels of DEGs identified in the comparison of LP_Liver vs. LCP_Liver. Table S4.7 Expression levels of DEGs identified in the comparison of LC_Liver vs. LPC_Liver. Table S4.8 Expression levels of DEGs identified in the comparison of LP_Liver vs. LPC_Liver. Table S4.9 The expression levels of DEGs identified in the comparison of LC_Muscle vs. LCP_Muscle. Table S4.10 The expression levels of DEGs identified in the comparison of LP_Muscle vs. LCP_Muscle. Table S4.11 The expression levels of DEGs identified in the comparison of LC_Muscle vs. LPC_Muscle. Table S4.12 Expression levels of DEGs identified in the comparison of LP_Muscle vs. LPC_Muscle.

Supplementary Material 4: Additional file 4: Fig. S1. GO and KEGG functional enrichment analyses of DEGs. a, b GO enrichment analysis of LCP and LPC DEGs; c, d KEGG pathway enrichment analyses of LCP and LPC DEGs.

Supplementary Material 5: Additional file 5: Table S5. The number of hyper and hypo-DMRs between hybrid lines and their parents.

Supplementary Material 6: Additional file 6: Fig. S2. DMR methylation level in CG contexts. Fig. S3. DMR methylation level in CHG contexts. Fig. S4. DMR methylation level in CHH contexts.

Supplementary Material 7: Additional file 7: Fig. S5. The number of DMEGs detected between hybrid yellow croaker and its parents. a-d LC_Brain vs. LCP_Brain, LP_Brain vs. LCP_Brain, LC_Brain vs. LPC_Brain, LP_Brain vs. LPC_Brain; e-h LC_Liver vs. LCP_Liver, LP_Liver vs. LCP_Liver, LC_Liver vs. LPC_Liver, LP_Liver vs. LPC_Liver; i-l LC_Muscle vs. LCP_Muscle, LP_Muscle vs. LCP_Muscle, LC_Muscle vs. LPC_Muscle, LP_Muscle vs. LPC_Muscle. Table S6. The DMEGs between the hybrid lines and their parents.

Supplementary Material 8: Additional file 8: Table S7. GO and KEGG annotation of DMEGs. Table S7.1 GO classification annotation of DMEGs. Table S7.2 KEGG pathway analysis of DMEGs.

Supplementary Material 9

Supplementary Material 10

Supplementary Material 11

Supplementary Material 12

Acknowledgements
Not applicable.

Author contributions
D.G. and B.L. conceived and designed the research. F.L. and F.W. participated in the reagents/materials preparation. D.G. analyzed the data. D.G. wrote the manuscript. Q.X., T.Y. and B.N. contributed to the data analysis. All the authors read and approved the final manuscript.

Funding
This research was supported by Zhejiang Provincial Natural Science Foundation of China under Grant No. LQN25C190002, the Key Scientific and Technological Grant of Zhejiang for Breeding New Agricultural (Aquaculture) Varieties (No. 2021C02069-1) and the Key Research and Development Project of Zhejiang Province (No. 2021C02055).

Data availability
The transcriptome and DNA methylation data from this study have been deposited in the NCBI Gene Expression Omnibus (GEO) under accession number GSE286334 and in the Genome Sequence Archive (GSA) under accession number CRA022045, respectively.

Declaration

Ethics approval and consent to participate
The study was performed according to the Guide for the Care and Use of Laboratory Animals of the National Advisory Committee for Laboratory Animal Research and guidelines approved by the Committee of Laboratory Animal Experimentation at the Zhejiang Academy of Agricultural Sciences.

Consent for publication
Not applicable.

Competing interests
The authors declare no competing interests.

Received: 15 April 2024 / Accepted: 15 January 2025
Published online: 12 February 2025

References

1. Liu SJ, Wang J, Luo KK, Xiao J, Qin QB, Tao M, Zhang C, Ren L. A novel high-quality variety of crucian carp derived from the crossbreeding of female white crucian carp and male red crucian carp. Current Fisheries. 2016;41(7):89.
2. Guo DD, Liu F, Niu BL, Zhan W, Xie QP, Zhang Y, Lou B. Establishment of diploid hybrid strains derived from female *Larimichthys crocea* × male *Larimichthys polyactis* and transmission of parental mtDNA in hybrid progenies. Aquaculture. 2022;561.
3. FBMA. Chinese fisheries Year Book. China:China Agriculture; 2013. p. 26.
4. Li Y, Han Z, Song N, Gao TX. New evidence to genetic analysis of small yellow croaker (*Larimichthys polyactis*) with continuous distribution in China. Biochem Syst Ecol. 2013;50:331–8.
5. Liang S. Physiological and molecular basis of cold and disease resistance heterosis in *Haliotis diversicolor* hybrid. Xiamen University; 2017.
6. Cao Y. Comparative analysis on genome-wide methylation and RNA-seq in Longissimus Dorsi Muscle between dorper × small tailed Han crossbred and small tailed Han Sheep. Jilin University; 2017.
7. Wang MY, Wang JB. Transcriptome and DNA methylome analyses provide insight into the heterosis in flag leaf of inter-subspecific hybrid rice. Plant Mol Biol. 2022;108(1–2):105–25.
8. Greaves IK, Groszmann M, Dennis ES, Peacock WJ. Trans-chromosomal methylation. Epigenetics. 2012;7(8):800–05.
9. Groszmann M, Greaves IK, Fujimoto R, Peacock WJ, Dennis ES. The role of epigenetics in hybrid vigour. Trends Genet. 2013;29(12):684–90.
10. Li RQ, Li YR, Kristiansen K, Wang J. SOAP: short oligonucleotide alignment program. Bioinformatics. 2008;24(5):713–14.
11. Kim D, Langmead B, Salzberg SL. HISAT: a fast spliced aligner with low memory requirements. Nat Methods. 2015;12(4):357–60.
12. Li B, Dewey CN. RSEM: accurate transcript quantification from RNA-Seq data with or without a reference genome. BMC Bioinformatics. 2011;12(1):323.
13. Love MI, Huber W, Anders S. Moderated estimation of Fold change and dispersion for RNA-seq data with DESeq2. Genome Biol. 2014;15(12):550.
14. Abdi H. The Bonferonni and Šidák corrections for multiple comparisons. Encyclopedia of Measurement and Statistics; 2007.
15. Krueger F, Andrews SR. Bismark: a flexible aligner and methylation caller for Bisulfite-Seq applications. Bioinformatics. 2011;27(11):1571–2.
16. Smallwood SA, Lee HJ, Angermueller C, Krueger F, Saadeh H, Peat J, Andrews SR, Stegle O, Reik W, Kelsey G. Single-cell genome-wide bisulfite sequencing for assessing epigenetic heterogeneity. Nat Methods. 2014;11(8):817–20.
17. Feng H, Conneely KN, Wu H. A bayesian hierarchical model to detect differentially methylated loci from single nucleotide resolution sequencing data. Nucleic Acids Res. 2014;42(8):e69.
18. Park YS, Wu H. Differential methylation analysis for BS-seq data under general experimental design. Bioinformatics. 2016;32(10):1446–53.
19. Wu H, Xu TL, Feng H, Chen L, Li B, Yao B, Qin ZH, Jin P, Conneely KN. Detection of differentially methylated regions from whole-genome bisulfite sequencing data without replicates. Nucleic Acids Res. 2015;43(21):e141.
20. Young MD, Wakefield MJ, Smyth GK, Oshlack A. Gene ontology analysis for RNA-seq: accounting for selection bias. Genome Biol. 2010;11(2):R14.
21. Mao XZ, Cai T, Olyarchuk JG, Wei LP. Automated genome annotation and pathway identification using the KEGG Orthology (KO) as a controlled vocabulary. Bioinformatics. 2005;21(19):3787–93.
22. Wei G, Tao Y, Liu GZ, Chen C, Luo RY, Xia HA, Gan Q, Zeng HP, Lu ZK, Han YN, et al. A transcriptomic analysis of superhybrid rice LYP9 and its parents. PNAS. 2009;106(19):7695–701.
23. The Gene Ontology Consortium. Expansion of the Gene Ontology knowledgebase and resources. Nucleic Acids Res. 2017;45(D1):D331–8.
24. Kanehisa M, Furumichi M, Tanabe M, Sato Y, Morishima K. KEGG: new perspectives on genomes, pathways, diseases and drugs. Nucleic Acids Res. 2017;45(D1):D353–61.
25. Gong DB, Tao M, Xu LH, Hu FZ, Wei ZH, Wang S, Wang YD, Liu QF, Wu C, Luo KK, et al. An improved hybrid bream derived from a hybrid lineage of *Megalobrama amblycephala* (♀) x *Culter alburnus* (♂). Sci China Life Sci. 2022;65(6):1213–21.
26. Liu QF. Studies on the heredity characteristic of white crucian carp (*Carassius auratus Cuvieri*) (♀) × red crucian carp (*Carassius auratus red var.*) (♂) and its genetic modification. Hunan Nornal University; 2018.
27. Ou M, Mao HH, Luo Q, Zhao J, Liu HY, Zhu XP, Chen KC. The DNA methylation level is associated with the superior growth of the hybrid fry in snakehead fish (*Channa argus* x *Channa maculata*). Gene. 2019;703:125–33.
28. Li H, Yuan JY, Wu M, Han ZP, Li LH, Jiang HM, Jia YL, Han XH, Liu ML, Sun DL, et al. Transcriptome and DNA methylome reveal insights into yield heterosis in the curds of broccoli (*Brassica oleracea* L var. *Italic*). BMC Plant Biol. 2018;18(1):168.
29. Guan WZ, Qiu GF, Liu F. Transcriptome analysis of the growth performance of hybrid mandarin fish after food conversion. PLoS ONE. 2020;15(10):e0240308.
30. Sun Y, Guo CY, Wang DD, Li XF, Xiao L, Zhang XH, You XX, Shi Q, Hu GJ, Fang C, et al. Transcriptome analysis reveals the molecular mechanisms underlying growth superiority in a novel grouper hybrid (*Epinephelus Fuscogutatus* ♀ x *E. Lanceolatus* ♂). BMC Genet. 2016;17:24.
31. Gao FX, Lu WJ, Shi Y, Zhu HY, Wang YH, Tu HQ, Gao Y, Zhou L, Gui JF, Zhao Z. Transcriptome profiling revealed the growth superiority of hybrid pufferfish derived from *Takifugu obscurus* ♀ x *Takifugu Rubripes* ♂. COMP BIOCHEM PHYS D. 2021;40:100912.
32. Ng DWK, Miller M, Yu HH, Huang TY, Kim ED, Lu J, Xie QG, McClung CR, Chen ZJ. A role for CHH methylation in the parent-of-origin effect on altered circadian rhythms and Biomass Heterosis in *Arabidopsis* Intraspecific hybrids. Plant Cell. 2014;26(6):2430–40.
33. Gao M, Huang QJ, Chu YG, Ding CJ, Zhang BY, Su XH. Analysis of the leaf methylomes of parents and their hybrids provides new insight into hybrid vigor in *Populus deltoides*. BMC Genet. 2014;15(Suppl 1):S8.
34. Cao Y, Jin HG, Ma HH, Zhao ZH. Comparative analysis on genome-wide DNA methylation in longissimus dorsi muscle between small tailed Han and Dorper x Small Tailed Han crossbred sheep. Asian-Australas J Anim Sci. 2017;30(11):1529–39.
35. Sun LF, Liu TJ, Shan XH, Su SZ, Li SP, Yuan YP, Zhang J. Analysis of DNA cytosine methylation patterns in maize hybrids and their parents. Biol Plant. 2015;59(2):266–72.
36. Shang HW, Liu ZG, Zhu HP, Gao FY, Ke XL, Lu MX. Analysis of DNA methylation difference between Mohe hybrid tilapia and its parents. J Fisheries China. 2017;44(11):1699–709.
37. Dedieu S, Mazeres G, Dourdin N, Cottin P, Brustis JJ. Transactivation of *capn2* by myogenic regulatory factors during myogenesis. J Mol Biol. 2003;326(2):453–65.
38. Cota D, Proulx K, Smith KAB, Kozma SC, Thomas G, Woods SC, Seeley RJ. Hypothalamic mTOR signaling regulates Food Intake. Science. 2006;312:917–30.
39. Shen XX, Zhao XY, He HR, Zhao J, Wei YH, Chen YQ, Han SS, Zhu YF, Zhang Y, Zhu Q, et al. Evolutionary conserved circular MEF2A RNAs regulate myogenic differentiation and skeletal muscle development. PLoS Genet. 2023;19(9):e1010923.
40. Lee CJ, An HJ, Cho ES, Kang HC, Lee JY, Lee HS, Cho YY. Stat2 stability regulation: an intersection between immunity and carcinogenesis. Exp Mol Med. 2020;52(9):1526–36.

Publisher's note